

# In-situ fabrication of a 3D-printed porous structure



K. Chen<sup>a</sup>, W. Li<sup>a</sup>, J. Li<sup>a,\*</sup>, L. He<sup>b</sup>, C. Wang<sup>c</sup>, Y. Li<sup>d</sup>, F. Li<sup>e</sup>, S. Wang<sup>f</sup>, K. E<sup>g</sup>, L. Li<sup>g</sup>, G. Li<sup>g</sup>, T. P. Jones<sup>f</sup>

<sup>a</sup> Gemmological Institute, China University of Geosciences, Wuhan 430074, PR China  
<sup>b</sup> Hubei Gem and Jewelry Engineering Technology Research Center, Wuhan 430074, PR China  
<sup>c</sup> School of Materials Science and Engineering, Huazhong University of Science and Technology, Wuhan 430074, PR China  
<sup>d</sup> Mechanical Engineering, University of Birmingham, Birmingham B15 2TT, UK  
<sup>e</sup> School of Electrical and Electronic Engineering, Huazhong University of Science and Technology, Wuhan 430074, PR China  
<sup>f</sup> WMG, Materials Engineering Centre, University of Warwick, CV4 7AL Coventry, UK

ARTICLE INFO

**Keywords:**  
 3D printing  
 porous structure  
 in-situ fabrication  
 mechanical properties

ABSTRACT

This paper presents a novel method for the in-situ fabrication of a porous structure using a 3D-printed mold. The porous structure is fabricated by the in-situ growth of a porous material within the mold. The porous structure is characterized by its porous structure and mechanical properties. The porous structure is fabricated by the in-situ growth of a porous material within the mold. The porous structure is characterized by its porous structure and mechanical properties. The porous structure is fabricated by the in-situ growth of a porous material within the mold. The porous structure is characterized by its porous structure and mechanical properties.

1. Introduction

The porous structure is a type of material with a porous structure. The porous structure is characterized by its porous structure and mechanical properties. The porous structure is fabricated by the in-situ growth of a porous material within the mold. The porous structure is characterized by its porous structure and mechanical properties. The porous structure is fabricated by the in-situ growth of a porous material within the mold. The porous structure is characterized by its porous structure and mechanical properties.

The porous structure is a type of material with a porous structure. The porous structure is characterized by its porous structure and mechanical properties. The porous structure is fabricated by the in-situ growth of a porous material within the mold. The porous structure is characterized by its porous structure and mechanical properties. The porous structure is fabricated by the in-situ growth of a porous material within the mold. The porous structure is characterized by its porous structure and mechanical properties.

\*Corresponding author. E-mail address: [lij@...](mailto:lij@...) (J. Li).

... T x ... (u, ...  
... 3DG W ... 3DG. B ...  
... H W ...  
... 17,18.  
... 3DG W ...  
... 19.  
... (SLM), ...  
... (AM) ...  
... (3D) ...  
... *in-situ* ...  
... SLM ...  
... 20,  
... 21, ... 22. C ...  
... C ...  
... CVD ...  
... (< 0.001 ...%) ...  
... 23. W ...  
... (> 0.1 ...%) 17, ...  
... 24. H W ...  
... SLM f ...  
... (1000-1100 ...). F ...  
... SLM ... 25.  
... T ...  
... 3DG/ ... (3DG/C) ...  
... SLM ... CVD ...  
... A W ...  
... SLM f ...



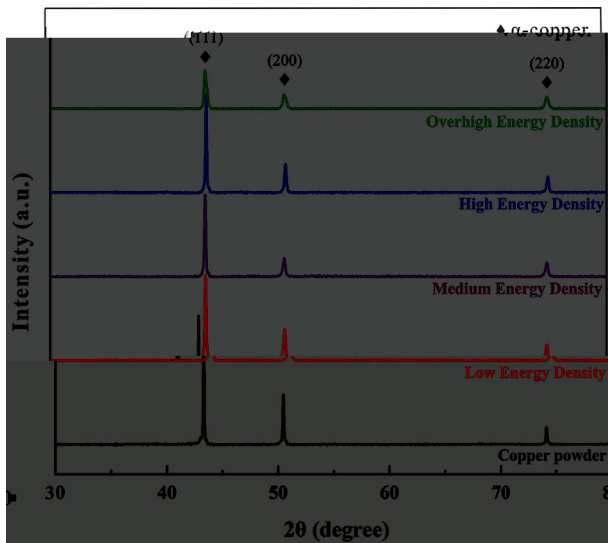


Fig. 3. RD patterns of copper powder at different energy densities. (a) 3000 J/mm<sup>3</sup>, (b) 857 J/mm<sup>3</sup>, (c) 285 J/mm<sup>3</sup>, (d) 128 J/mm<sup>3</sup>, (e) copper powder.

3.1.2. Formation of anisotropic microstructure under different volumetric energy density

The XRD patterns of copper powder at different energy densities are shown in Fig. 3. The (111) peak is the most prominent in all samples, indicating a strong texture along the [111] direction. The intensity of the (111) peak increases with increasing energy density, while the intensity of the (200) and (220) peaks decreases. This suggests that higher energy density leads to a more pronounced anisotropic microstructure. The copper powder reference pattern is also shown for comparison.

The XRD patterns of copper powder at different energy densities are shown in Fig. 3. The (111) peak is the most prominent in all samples, indicating a strong texture along the [111] direction. The intensity of the (111) peak increases with increasing energy density, while the intensity of the (200) and (220) peaks decreases. This suggests that higher energy density leads to a more pronounced anisotropic microstructure. The copper powder reference pattern is also shown for comparison.

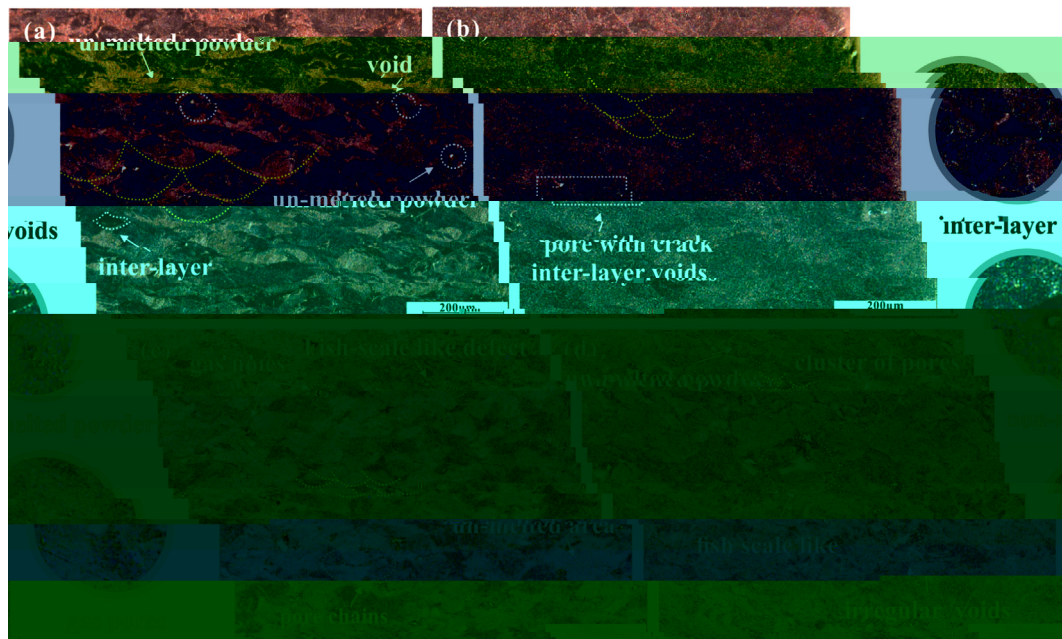


Fig. 4. SEM micrographs of SLM copper powder at different energy densities: (a) 3000 J/mm<sup>3</sup>, (b) 857 J/mm<sup>3</sup>, (c) 285 J/mm<sup>3</sup>, (d) 128 J/mm<sup>3</sup>. (Figs. 4a-d) show the surface morphology of the SLM copper powder at different energy densities. (a) shows un-melted powder, voids, and inter-layer voids. (b) shows a pore with crack and inter-layer voids. (c) and (d) show smooth surfaces.







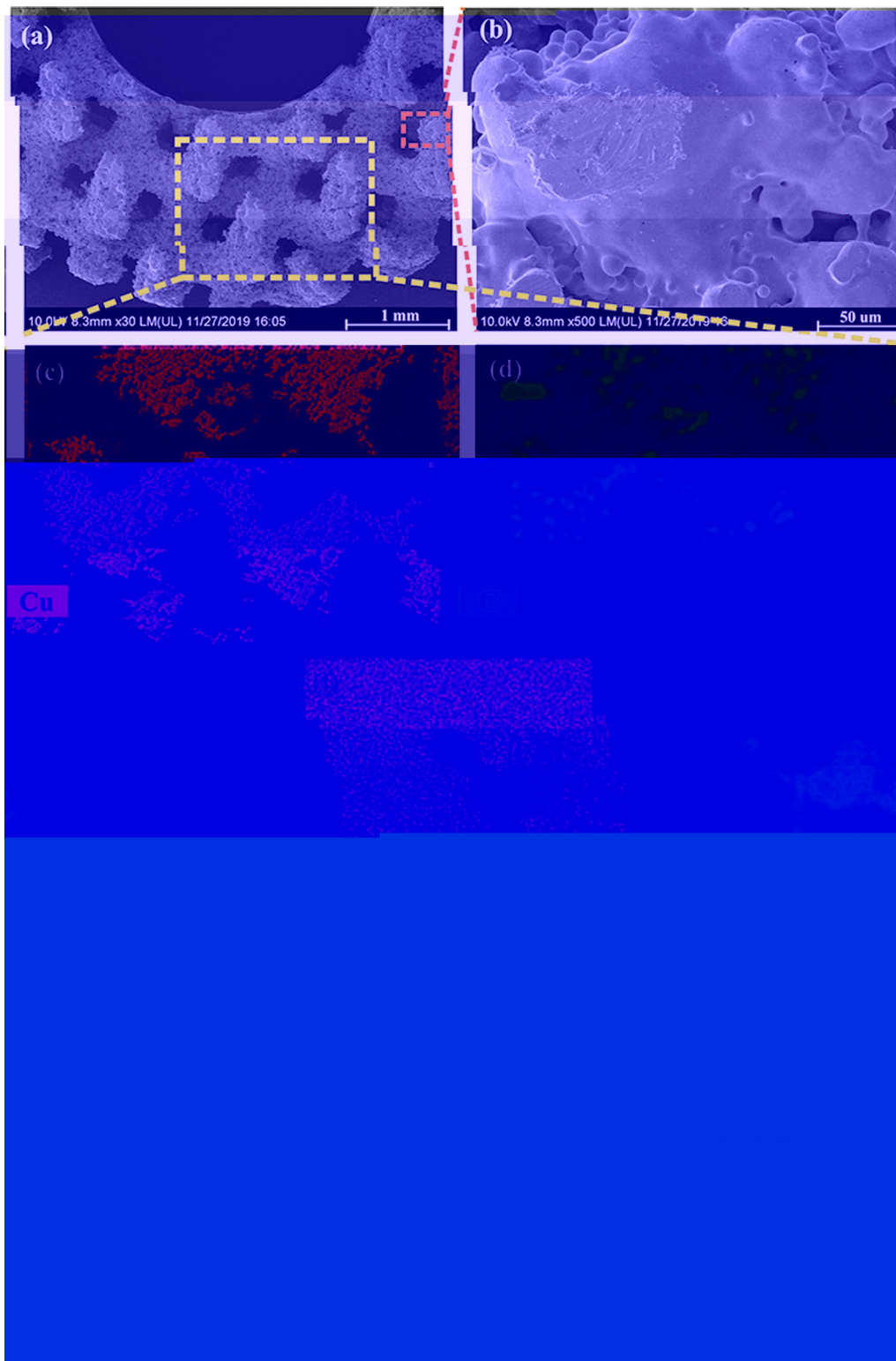


Fig. 8. (a) SEM image of 3DG/Cu porous scaffold; (b) SEM image of 3DG/Cu porous scaffold; (c) EDS map of 3DG/Cu porous scaffold; (d) EDS map of 3DG/Cu porous scaffold. (e) EDS map of 3DG/Cu porous scaffold.

SEM image of 3DG/Cu porous scaffold. The image shows a porous structure with interconnected pores. The scale bar is 1 mm. The SEM image of 3DG/Cu porous scaffold at 50 μm scale shows a detailed view of the porous structure. The EDS map of 3DG/Cu porous scaffold shows the distribution of elements. The EDS map of 3DG/Cu porous scaffold shows the distribution of elements. The EDS map of 3DG/Cu porous scaffold shows the distribution of elements.

### 3.4. Thermal property and EMI shielding effectiveness of 3DG/Cu porous scaffolds

The thermal property and EMI shielding effectiveness of 3DG/Cu porous scaffolds were investigated. The results are shown in Table 1. The thermal conductivity of 3DG/Cu porous scaffold is 0.71 W/mK. The EMI shielding effectiveness of 3DG/Cu porous scaffold is 26.8% at 1000 MHz and 14.8% at 10 MHz.

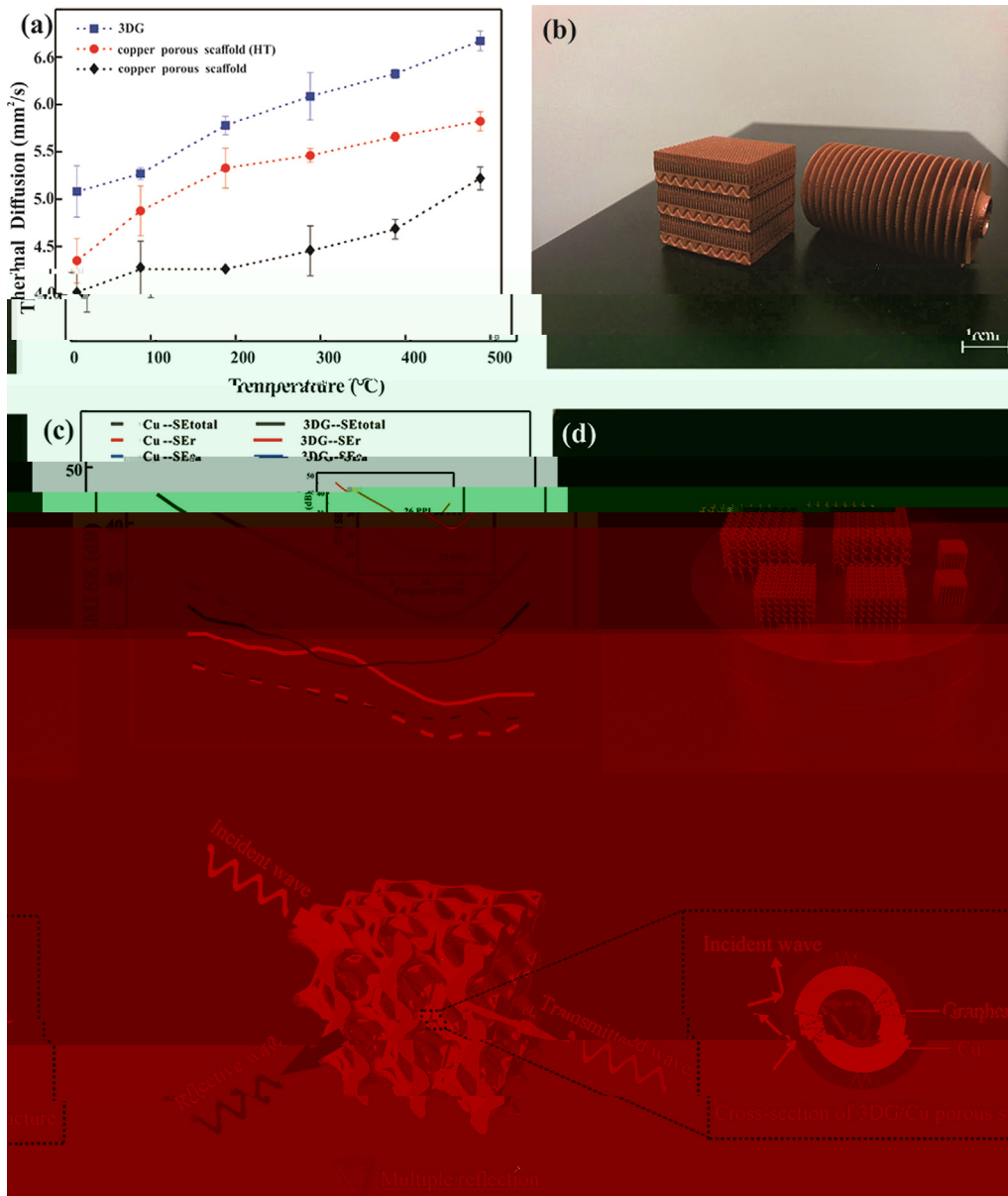


Fig. 9. (a) Thermal Diffusion of 3DG/Cu porous scaffold. (b) Photograph of 3DG and copper porous scaffold samples. (c) SEM image of the 3DG/Cu porous scaffold structure. (d) Schematic diagram of the EM wave shielding mechanism showing incident, reflected, and transmitted waves, and multiple reflections within the porous structure.

Table 1  
Comparison of the maximum shielding efficiency and improvement of thermal property for various EM wave shielding materials.

Coating materials	Substrate	Method	Maximum shielding efficiency (dB)	Improvement of thermal property (%)	Ref
G <sup>1</sup>	G <sup>1</sup>	SLM	37	-	50
G <sup>1</sup>	PS	SLM	29.3	-	56
G <sup>1</sup>	PMMA	SLM	19	-	57
C/G <sup>1</sup>	Al	SLM	-	8.5	58
G <sup>1</sup>	Ni	SLM + CVD	-	554	59
G <sup>1</sup>	C-Ni	SLM	20	-	60
G <sup>1</sup>	C	SLM + CVD	-	2.4	61
G <sup>1</sup>	C	SLM	47	6.3	62
G <sup>1</sup>	C	CVD + SLM	47.8	27	63

Note: (a) 3DG/Cu porous scaffold; (b) 3DG/Cu porous scaffold; (c) 3DG/Cu porous scaffold; (d) 3DG/Cu porous scaffold.







